Hindawi
International Journal of Photoenergy
Volume 2017, Article ID 9628146, 8 pages
https://doi.org/10.1155/2017/9628146

Research Article

Protonation and Photocatalytic Activity of the $Rb_2La_2Ti_3O_{10}$ Layered Oxide in the Reaction of Hydrogen Production

Ivan A. Rodionov, Iuliia P. Sokolova, Oleg I. Silyukov, Alena A. Burovikhina, Sergey A. Fateev, and Irina A. Zvereva

Saint Petersburg State University, 7-9 Universitetskaya nab, St. Petersburg 199034, Russia

Correspondence should be addressed to Ivan A. Rodionov; i.rodionov@spbu.ru

Received 10 August 2017; Revised 2 October 2017; Accepted 29 October 2017; Published 20 December 2017

Academic Editor: Yanfa Yan

The $Rb_2La_2Ti_3O_{10}$ layered oxide was synthesized by the solid-state method. Three phases with different protonation degrees and intercalated water contents were obtained from the initial compound by the treatment with distilled water and hydrochloric acid. The obtained samples were characterized by powder X-ray diffraction, SEM, X-ray microanalysis, BET, DRS, and TG. It was found that the complete ion exchange of Rb^+ for H^+ in the layered oxide $Rb_2La_2Ti_3O_{10}$ proceeds through the formation of two metastable intermediate phases with average protonation degrees of 0.5 and 0.75, which successively transform from one to another. Each of these phase transformations is accompanied not only by the contraction of the interlayer distance but also by the displacement of adjacent perovskite layers by 1/2 of the cell parameter which results in the change in the space group. The photocatalytic activity of obtained samples decreases with the increase in the protonation degree, which correlates with the decrease in the intercalated water content.

1. Introduction

Photocatalytic production of hydrogen from renewable resources such as water or biomass is regarded as a promising way to deal with the problems of exhaustion of traditional fuel feedstocks and the environment pollution caused by their use [1, 2]. Many inorganic materials were proposed as photocatalysts for hydrogen production under UV and visible light irradiation [3–5]. Layered oxides represent a unique class of photocatalysts, which have the abilities to intercalate substrate molecules into the interlayer space, to exchange interlayer cations for different structural units and to undergo the exfoliation process with the formation of oxide nanosheets [6]. These properties already allowed creating highly efficient photocatalytic systems and open-wide possibilities in the future [7].

The $A_2La_2Ti_3O_{10}$ (A = alkaline metal) oxides belong to the triple-layered Ruddlesden-Popper perovskite-like titanates. The photocatalytic activity of $K_2La_2Ti_3O_{10}$ in the reaction of water splitting under UV light was first reported by Takata et al. [8]. The high activity was explained by the possibility of the water molecules intercalated in the interlayer space to take part in the photocatalytic reaction. Takata et al. [9] attempted to confirm this mechanism for the isostructural titanate $Rb_2La_2Ti_3O_{10}$, which demonstrated an activity twice as high as the potassium-containing analogue. It was found that the partial substitution of Ti with Nb results in the loss of intercalation ability and a significant decrease in the photocatalytic activity. Moreover, isostructural layered oxides $Li_2La_2Ti_3O_{10}$ and $Na_2La_2Ti_3O_{10}$, which do not intercalate water at ambient conditions, show very low efficiency in the reaction of hydrogen production under UV light [10, 11]. Thus, the photocatalytic activity of triple-layered titanates $A_2La_2Ti_3O_{10}$ is likely to be connected with their intercalation ability, which is also the case for some other layered oxides [12, 13].

During the past years, the $K_2La_2Ti_3O_{10}$ layered oxide has become a popular research object as a photocatalyst [7], but, surprisingly, $Rb_2La_2Ti_3O_{10}$ did not, despite that it has initially demonstrated much higher photocatalytic

performance. This fact may be associated with a higher cost of rubidium in comparison with potassium. Anyway, we could not find any reports about photocatalytic properties of $Rb_2La_2Ti_3O_{10}$ since the original work [8], in contrast with $K_2La_2Ti_3O_{10}$, which was investigated in more than 60 papers. These works cover a wide range of research directions devoted to the enhancement of photocatalytic properties, including improved synthesis techniques, doping, and design of composite photocatalysts. Nevertheless, we believe that there is a lack in these investigations, namely, the study of reactions between the layered oxide and aqueous solution.

It is a matter of common knowledge that many layered oxides undergo protonation, that is, substitution of interlayer cations for protons in acidic solution [14]. The protonation process is a widely used technique in soft chemistry of layered oxides and is a starting point for many synthetic routes [6]. However, there is a nonobvious fact that layered oxides may undergo protonation not only in acidic but also in neutral and even alkaline aqueous solution. Since the protonation process changes the structure of the interlayer space and affects the intercalation ability of the layered oxide, it may also have a dramatic impact on its photocatalytic properties. Unfortunately, this fact is usually overlooked in papers concerning the photocatalytic activity of $A_2La_2Ti_3O_{10}$-type titanates.

This paper is focused on the detailed study of protonation processes, which occur under contact of the $Rb_2La_2Ti_3O_{10}$ layered oxide with water and acidic solution, and their influence on its photocatalytic activity.

2. Materials and Methods

The layered oxide $Rb_2La_2Ti_3O_{10}$ was prepared by conventional solid-state reaction (1) in air at atmospheric pressure using Rb_2CO_3, La_2O_3, and TiO_2 as reagents (99.9%). The stoichiometric amounts of oxides with 50% excess of rubidium carbonate were ground in an agate mortar together with heptane to prevent hydration. Then, the mixture was pelletized by pressure and heated in a corundum crucible at 1000°C for 10 h.

$$La_2O_3 + 3TiO_2 + Rb_2CO_3 \rightarrow Rb_2La_2Ti_3O_{10} + CO_2\uparrow \quad (1)$$

The as-prepared sample is denoted as S0. The synthesis of protonated samples was carried out by the treatment of the initial sample S0 with distilled water and 0.01 M HCl. During this procedure, two main approaches were used. At the first stage, 5 g of the S0 sample was placed into a closed flask together with 40 ml of distilled water. The suspension was shaken for 10 min and centrifuged at 1000g. Finally, the fugate was replaced by fresh water, and the whole procedure was repeated 24 times until a single-phase product (S1) was obtained. At the second stage, the S1 sample was placed on a vacuum filter (average pore diameter 50 nm) and distilled water was added to it dropwise at an average rate of 5 ml/min by a peristaltic pump (Watson-Marlow-400) and continuously removed through the filter. After passing of 6 l of water through the filter, another single-phase product (S2) with a higher protonation degree was obtained. Finally, water was replaced by a 0.01 M HCl solution, and the S2 sample was exposed to it on the vacuum filter. After passing of 4.5 l of acid through the filter, the final product (S3) was obtained.

The phase composition of the obtained samples was determined by powder XRD (Rigaku Miniflex II, CuKα). The indexing of XRD patterns and determination of cell parameters were performed on Topas software provided by Bruker.

The degree of protonation as well as the amount of intercalated water was determined by thermogravimetric analysis (TG) (Netzsch TG 209 F1 Libra), which was performed in argon atmosphere with a heating rate of 10 K/min from room temperature to 800°C. Typically, two steps of mass loss were observed on the TG curve. The first step (80–250°C) corresponds to the liberation of intercalated water and the second step (300–400°C) refers to the dehydration of the partly protonated layered oxide as follows:

$$H_xRb_{2-x}La_2Ti_3O_{10} \cdot yH_2O = H_xRb_{2-x}La_2Ti_3O_{10} + yH_2O$$
$$H_xRb_{2-x}La_2Ti_3O_{10} = Rb_{2-x}La_2Ti_3O_{10-(x/2)} + \frac{x}{2}H_2O \quad (2)$$

The values $x/2$ (protonation degree) and y (amount of intercalated water per formula unit) were calculated on the basis of these equations [15].

The morphology of the samples was investigated by scanning electron microscopy (Zeiss Merlin with field emission cathode, electron optics column GEMINI-II, and oil-free vacuum system). Furthermore, energy-dispersive X-ray microanalysis of the samples was carried out (Oxford Instruments INCAx-act), and the protonation degree was calculated from the relative rubidium content in each sample.

The specific surface area of the samples was determined using the Brunauer-Emmett-Teller (BET) method (Quadrasorb SI) by measuring the amount of adsorbed krypton.

The optical band gap energy of the samples was determined by diffuse reflectance spectroscopy (DRS) (Shimadzu UV-2550 with ISR-2200 integrating sphere attachment). The band gap was determined from the crosspoint of linear sections of the Kubelka-Munk function (F) plot in the coordinates $(F \cdot h\nu)^{1/2} = f(h\nu)$.

To prepare the suspension for the photocatalytic experiment, 60 mg of the photocatalyst sample was added to 60 ml of aqueous solution containing 0.1% (mol) isopropyl alcohol and, in some experiments, 0.1 M KOH in order to maintain the pH constant. The suspension was shaken and left for 1 hour to establish equilibrium between the photocatalyst and solution. Straight before the experiment, each suspension was sonicated for 10 min (Elmasonic S10H ultrasound bath) to disaggregate the photocatalyst particles. The pH of each suspension was measured by a Mettler Toledo S220 SevenCompact pH meter equipped with an InLab Expert Pro-ISM electrode.

The photocatalyst suspension (50 ml) was placed in an external irradiation reaction cell, equipped with a powerful magnetic stirrer and a liquid cut-off filter and connected to

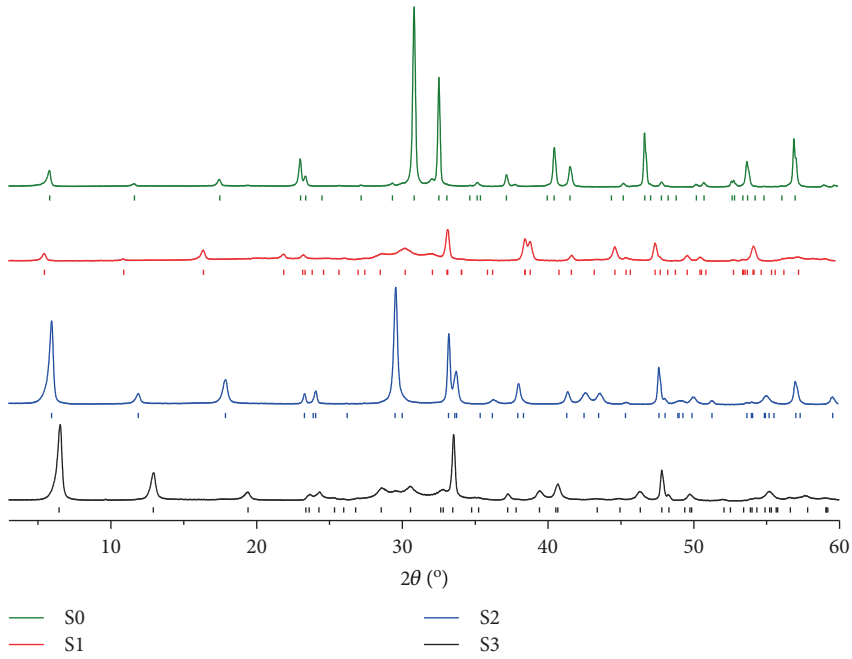

Figure 1: X-ray powder diffraction patterns of the initial (S0) and protonated (S1, S2, and S3) $Rb_2La_2Ti_3O_{10}$ samples.

a closed gas circulation system (120 ml dead volume). A medium-pressure mercury lamp DRT-125 (125 W) was used as a radiation source. Light reaches the reaction cell only after passing through a thermostated light filter solution at 15°C (KCl + NaBr, 6 g/l each, 2 cm optical path), which cuts off radiation with $\lambda < 220$ nm. The total irradiation time was 120 min for each experiment. During the photocatalytic reaction, hydrogen accumulates in the gas phase, whose composition was analyzed by an online gas chromatograph at certain time intervals (Shimadzu GC-2014, Rt-Msieve 5A Column, TCD, Ar carrier). At the beginning of each experiment, the system was deaerated and argon gas was introduced at atmospheric pressure.

3. Results and Discussion

The initial $Rb_2La_2Ti_3O_{10}$ sample (S0) was synthesized as a single phase without impurities; the obtained XRD pattern (Figure 1) is consistent with that in literature data [16] and corresponds to an I4/mmm space group with cell parameters $a = 3.895$ Å and $c = 30.46$ Å. When we exposed the S0 sample to liquid water, we detected two main processes: the intercalation of water molecules into the interlayer space and the exchange of interlayer rubidium cations for protons. These processes are accompanied by phase transformations, that is, we observe the disappearance of initial peaks and appearance of new peaks on the XRD patterns instead of a continuous shift of the lattice parameters. Moreover, we discovered that there exists not only the fully protonated phase $H_2La_2Ti_3O_{10}$, which is described in literature, but also partially protonated phases with different space groups. During the treatment of the initial sample with water, we managed to obtain two intermediate phases S1 and S2 with different protonation degrees and different contents of intercalated water. Furthermore, by means of treatment of the S2 sample with 0.01 M HCl, we obtained the S3 sample, which was fully protonated.

According to TG data (Figure 2 and Table 1), the sample S1 has the composition $HRbLa_2Ti_3O_{10}\cdot 0.8H_2O$, that is, half of the rubidium ions are substituted with protons. The peaks on the XRD pattern of S1 have lower intensity compared to those of the initial S0 sample, and some of them are broadened (especially in the 28°–33° region). This may be due to the structural disorder (i.e., stacking disorder), caused by the displacement of perovskite layers during the ion exchange and intercalation processes. The XRD pattern of S1 can be well indexed in an orthorhombic space group C222 with $a = b = 3.84$ Å and $c = 32.52$ Å, which corresponds to the displacement of adjacent perovskite slabs in one direction (a or b) by 1/2 of the cell parameter compared to the I4/mmm space group of S0.

Sample S2 has a higher protonation degree and a less content of intercalated water as compared to S1. Its composition can roughly be described as $H_{1.5}Rb_{0.5}La_2Ti_3O_{10}\cdot 0.5H_2O$. In contrast with S1, it is well crystallized and its XRD pattern is perfectly indexed in a P4/mmm space group with $a = 3.82$ Å and $c = 14.90$ Å, corresponding to an eclipsed configuration of adjacent perovskite layers. Therefore, the S1 sample not only changes its composition during flushing with 6 l of distilled water but also transforms it into a more symmetric and ordered form—S2.

Sample S3 is almost completely protonated and contains a minor amount of water. TG data show that in this case, water desorbs at lower temperature compared to that of S1 and S2, suggesting that it may be physically adsorbed rather than intercalated. The formula of S3 can be written as $H_{1.9}Rb_{0.1}La_2Ti_3O_{10}\cdot 0.16H_2O$. Compared to S2, it has a lower structure symmetry and its XRD pattern can be described by

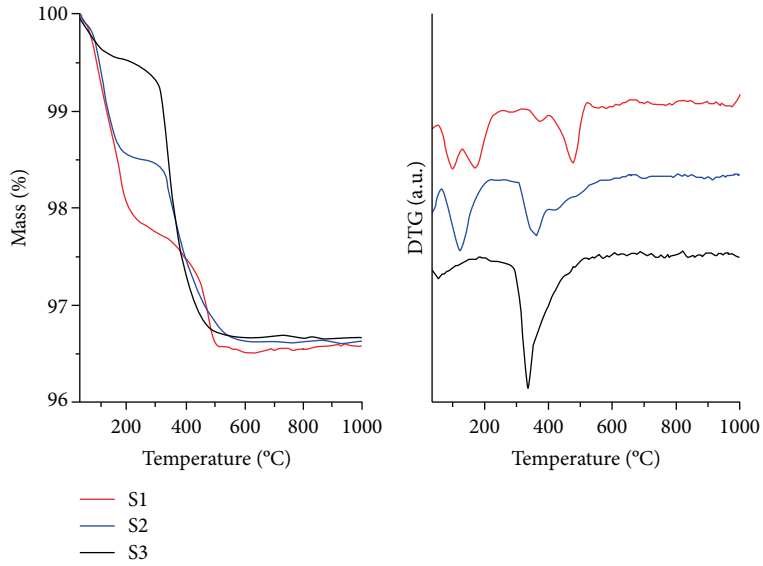

Figure 2: Thermogravimetric curves of protonated $Rb_2La_2Ti_3O_{10}$ samples S1, S2, and S3.

Table 1: Characteristics of obtained $Rb_2La_2Ti_3O_{10}$ samples S0, S1, S2, and S3: interlayer distance, protonation degree measured by TG and X-ray microanalysis, intercalated water content, and BET surface area.

	Space group	Interlayer distance (Å)	Substitution degree of K^+ with H^+ (%)		Amount of intercalated water per formula unit	Optical band gap (eV)	BET surface area (m^2/g)
			TG	X-ray microanalysis			
S0	I4/mmm	15.23	—	0	0	3.60	1.4
S1	C222	16.26	0.48	0.52	0.82	3.65	7.1
S2	P4/mmm	14.90	0.68	0.76	0.54	3.58	7.8
S3	C222	13.72	0.95	0.97	0.16	3.55	8.1

the orthorhombic space group C222 with $a = b = 3.805$ Å and $c = 27.44$ Å, which again corresponds to the displacement of adjacent perovskite slabs in one direction (a or b) by 1/2 of the cell parameter as well as in the case of S1. We can claim that this main phase of S3 is fully protonated, because the observed residual rubidium content is apparently related to the minor impurity of the S2 phase, which can be detected on the XRD pattern at 29.55°.

During the protonation process, we observe the decrease in the interlayer distance, which is related to the c lattice parameter. This is caused by two factors. On the one hand, bulky rubidium cations are replaced by compact protons. On the other hand, the amount of intercalated water also decreases. DRS experiments showed that the change in the interlayer distance correlates with the change in the band gap. The measured values of the band gap lie within the range of 3.55–3.65 eV (Figure 3) which is in general agreement with literature data [9]. It can be seen that the band gap energy increases in the series S3 < S2 < S0 < S1, in the same order as the interlayer distance (Table 1). The valence band and conductance band of layered titanates are formed mainly by O2p and Ti3d orbitals within the perovskite layer. The contribution of the alkali cation to the band formation in such compounds is usually negligible, so its nature should not have much impact on the band gap [17]. However, the band

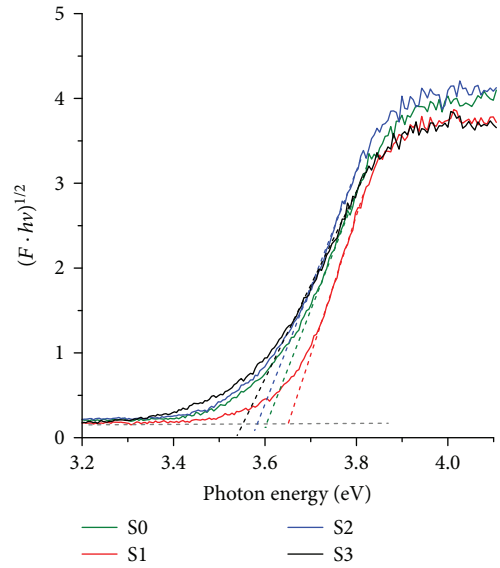

Figure 3: Transformed diffuse reflectance spectra of the initial (S0) and protonated (S1, S2, and S3) $Rb_2La_2Ti_3O_{10}$ samples.

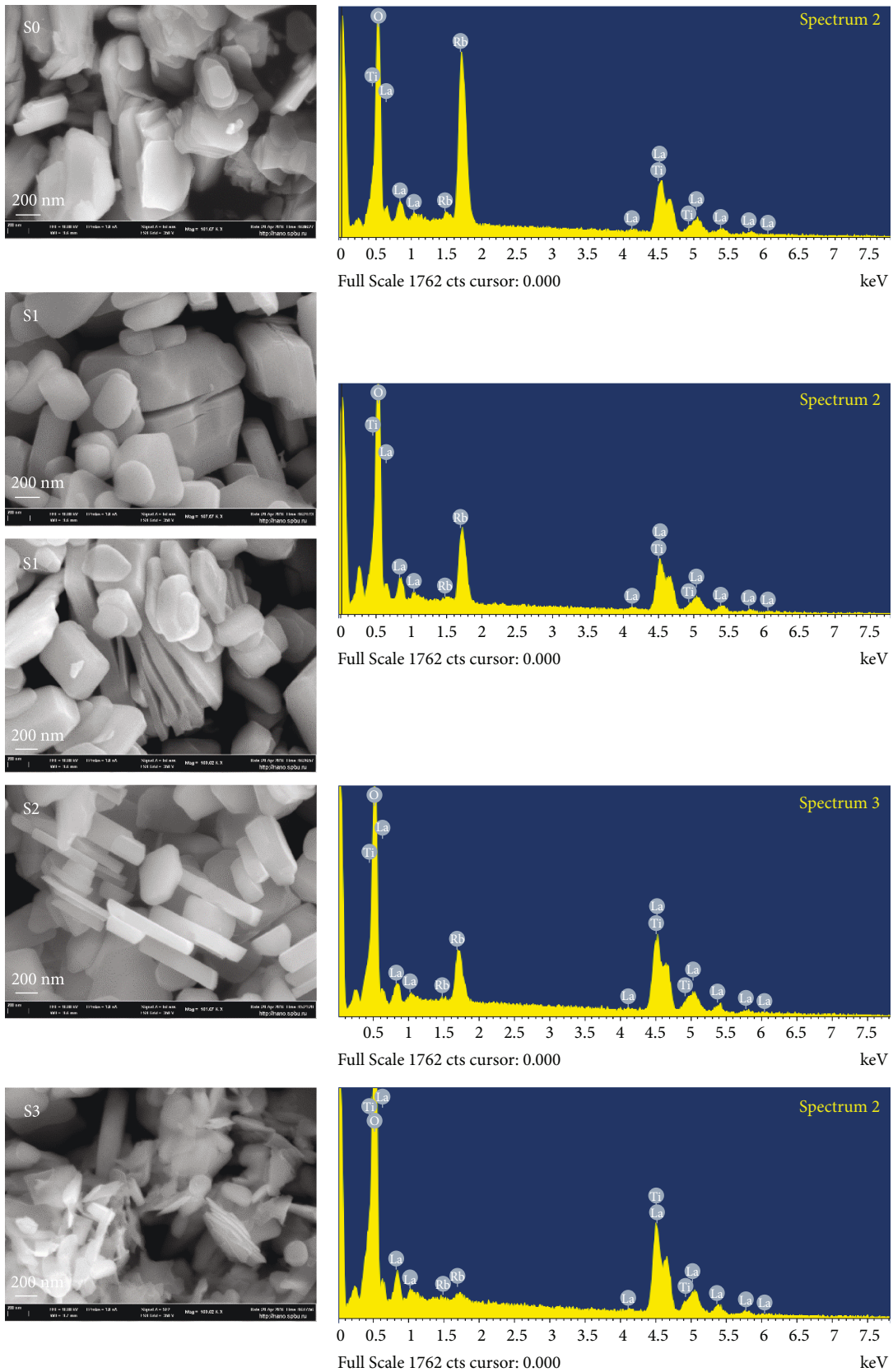

Figure 4: SEM images and X-ray microanalysis of obtained samples S0, S1, S2, and S3.

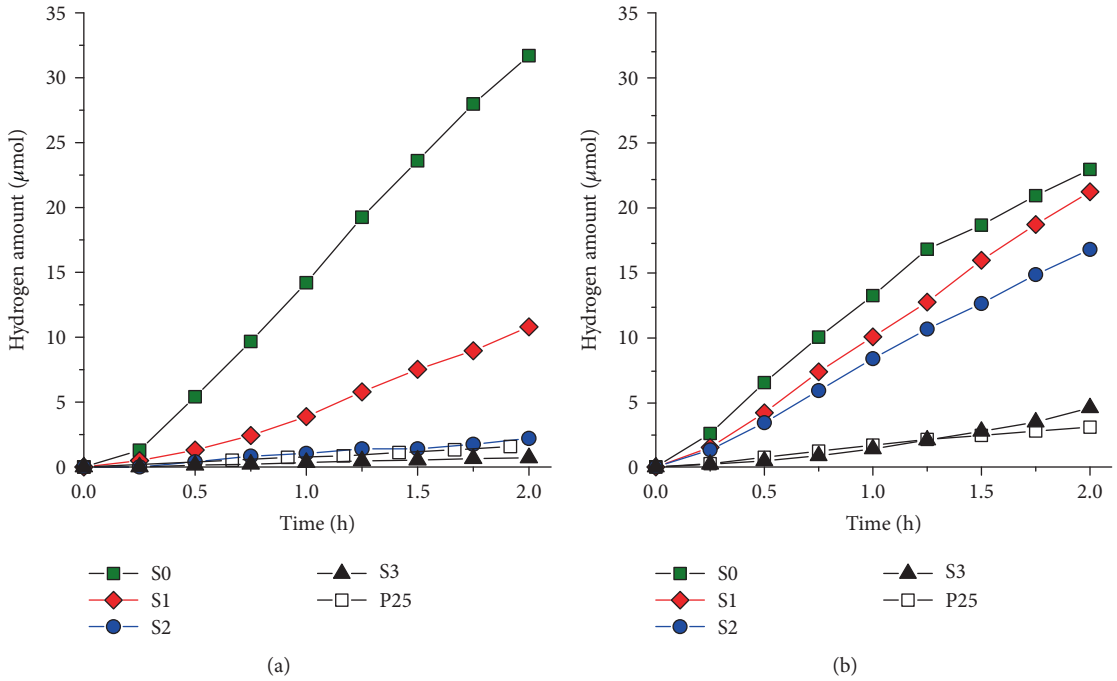

Figure 5: Kinetic curves of hydrogen evolution over $Rb_2La_2Ti_3O_{10}$ samples S0, S1, S2, S3, and TiO_2 P25 from 0.1% (mol) aqueous isopropanol solution in water (a) and 0.1 M KOH (b).

gap depends on the interaction between orbitals of adjacent perovskite layers, which clearly depends on the interlayer distance, explaining the observed correlation. The variation of the band bap among investigated samples is not critical, but it may have an impact on the photocatalytic activity due to the change in the electron and hole reactivity.

We have demonstrated that the interaction of $Rb_2La_2Ti_3O_{10}$ with water successively yields two metastable phases S1 and S2 with different protonation degrees, different contents of intercalated water, and even different structures. However, the observed phase transformations are accompanied by even more complex effects, namely, the increase in the specific surface area due to partial delamination of the layered oxide particles. These changes in morphology can be observed on the SEM images of the samples S0–S3 (Figure 4). While the initial sample S0 consists of bulky plate-like particles, for S1, we clearly observe fissures, which divide the particles into thinner units. The particles of the S2 and S3 samples, whose morphology is the result of this delamination process, have less thickness compared to those of S0, which results in the increased surface area. The BET surface area of all protonated samples exceeds that of the initial compound more than fivefold (Table 1). Hence, we could expect from the protonated samples an increased photocatalytic activity. However, experiments showed quite the contrary.

According to Figure 5, the photocatalytic activity of the layered oxide samples gradually decreases with the increase in the protonation degree in the series S0-S1-S2-S3. The superior activity was demonstrated by the initial S0 sample in the aqueous isopropanol solution without KOH. Under these conditions, its activity is ≈22 times larger than that of

Table 2: Photocatalytic activity of the obtained $Rb_2La_2Ti_3O_{10}$ samples S0, S1, S2, S3, and TiO_2 P25.

	Photocatalytic hydrogen evolution rate (μmol/h)		pH of the reacting suspension	
	In water	In 0.1 M KOH	In water	In 0.1 M KOH
S0	17.7	14.3	11.0	12.9
S1	6.1	11.6	9.9	12.9
S2	1.2	9.1	7.1	12.9
S3	0.4	2.5	5.3	12.9
P25	0.8	1.6	5.8	12.9

TiO_2 P25 Evonic-Degussa which was used for reference. The samples S2 and S3 show a quite low photocatalytic activity. Besides other reasons, this may be caused by the strong difference of the suspension pH (Table 2), which is in this case determined only by the equilibrium between the layered oxide and the solution (hydrolysis or dissociation).

At the same time, in the presence of KOH, the difference in the photocatalytic activity is not such critical. In this case, the pH is maintained constant. But, on the other hand, the protonated forms should be not stable at such alkaline pH values as they can act as solid acids. Protons in the interlayer space may become substituted by potassium ions from the solution, and this process is promoted by the neutralization reaction in an alkaline medium. The XRD pattern of protonated phases did not show significant changes after photocatalytic experiments. But even if the reverse ion exchange proceeds slowly and only at the surface of layered oxide particles, it may significantly affect the photocatalytic properties.

Maybe, this is the reason for the fact that the hydrogen evolution rate over the S3 sample slowly increases with irradiation time. Generally, we should note the correlation between photocatalytic activity and the amount of intercalated water in the interlayer space. Apparently, this is the reason why the initial sample, which is most capable of water intercalation, demonstrates the best photocatalytic performance in both cases.

To conclude, we would like to focus on the practical importance of the obtained results. When the layered oxide is used as a matrix for the creation of nanostructured composite photocatalysts, reactions of intercalation and ion exchange are usually involved in the preparation process. However, the optimal synthesis conditions as well as the quality of obtained product should strongly depend on the composition and structure of the initial layered oxide. We have shown that the $Rb_2La_2Ti_3O_{10}$ layered titanate forms three different protonated phases depending on the external conditions. These phases possess a different interlayer distance and a different amount of intercalated water; thus, most likely, their reactivity in ion exchange and intercalation processes should be different. Therefore, it is important to control which exactly protonated phase is involved in the reaction, when the layered oxide is taken as a starting compound. In the current paper, we have reported for the first time the existence of two intermediate protonated forms of $Rb_2La_2Ti_3O_{10}$ and characterized them. We hope that these results will be useful for the design of new materials based on layered oxides, especially high-performance photocatalysts.

4. Conclusions

It was found that the $Rb_2La_2Ti_3O_{10}$ layered oxide is not stable against rubidium leaching in aqueous solution. Two partially protonated phases of $Rb_2La_2Ti_3O_{10}$ were obtained and characterized for the first time. The intermediate phases with compositions $HRbLa_2Ti_3O_{10}{\cdot}0.8H_2O$ and $H_{1.5}Rb_{0.5}La_2Ti_3O_{10}{\cdot}0.5H_2O$ were obtained by washing the initial sample with distilled water, while the final fully protonated phase was obtained by the treatment with 0.01 M hydrochloric acid. With the increase in the protonation degree, we observed the decrease in intercalated water amount and the contraction of the interlayer distance. Each phase transformation between protonated forms is accompanied by the displacement of adjacent perovskite layers by 1/2 of the cell parameter. Partial delamination of the layered oxide particles occurred during the protonation of $Rb_2La_2Ti_3O_{10}$ resulting in an increase in the BET surface area. The photocatalytic activity decreases with the increase in the protonation degree, which correlates with the decrease in the intercalated water content. The initial nonprotonated layered oxide demonstrated the highest hydrogen production rate under UV irradiation.

Conflicts of Interest

The authors declare that there is no conflict of interest regarding the publication of this paper.

Acknowledgments

This research was supported by the Russian Foundation for Basic Research. Ivan A. Rodionov is grateful to the Grant no. 16-33-60044 and Oleg I. Silyukov acknowledges the Grant 16-33-60082. Ivan A. Rodionov is also grateful for the scholarship of the president of the Russian Federation (SP-2176.2016.1). The authors are grateful to the Saint Petersburg State University Research Park. TG studies were carried out in the Center of Thermal Analysis and Calorimetry, XRD studies were carried out in the Research Centre for X-ray Diffraction Studies, ICP-AES studies were carried out in the Centre for Chemical Analysis and Materials Research, SEM images were obtained in the Interdisciplinary Resource Centre for Nanotechnology, and the GC for photocatalytic experiments was provided by the Chemistry Educational Centre.

References

[1] A. V. Puga, "Photocatalytic production of hydrogen from biomass-derived feedstocks," *Coordination Chemistry Reviews*, vol. 315, pp. 1–66, 2016.

[2] J. O. Bockris, "Hydrogen economy in the future," *International Journal of Hydrogen Energy*, vol. 24, no. 1, pp. 1–15, 1999.

[3] F. E. Osterloh, "Inorganic materials as catalysts for photochemical splitting of water," *Chemistry of Materials*, vol. 20, no. 1, pp. 35–54, 2008.

[4] K. Maeda, "Photocatalytic water splitting using semiconductor particles: history and recent developments," *Journal of Photochemistry and Photobiology C Photochemistry Reviews*, vol. 12, no. 4, pp. 237–268, 2011.

[5] A. Kudo and Y. Miseki, "Heterogeneous photocatalyst materials for water splitting," *Chemical Society Reviews*, vol. 38, no. 1, pp. 253–278, 2009.

[6] R. E. Schaak and T. E. Mallouk, "Perovskites by design: a toolbox of solid-state reactions," *Chemistry of Materials*, vol. 14, no. 4, pp. 1455–1471, 2002.

[7] I. A. Rodionov and I. A. Zvereva, "Photocatalytic activity of layered perovskite-like oxides in practically valuable chemical reactions," *Russian Chemical Reviews*, vol. 85, no. 3, pp. 248–279, 2016.

[8] T. Takata, K. Shinohara, A. Tanaka, M. Hara, J. N. Kondo, and K. Domen, "A highly active photocatalyst for overall water splitting with a hydrated layered perovskite structure," *Journal of Photochemistry and Photobiology A: Chemistry*, vol. 106, no. 1-3, pp. 45–49, 1997.

[9] T. Takata, Y. Furumi, K. Shinohara et al., "Photocatalytic decomposition of water on spontaneously hydrated layered perovskites," *Chemistry of Materials*, vol. 9, no. 5, pp. 1063-1064, 1997.

[10] I. A. Rodionov, O. I. Silyukov, T. D. Utkina, M. V. Chislov, Y. P. Sokolova, and I. A. Zvereva, "Photocatalytic properties and hydration of perovskite-type layered titanates $A_2Ln_2Ti_3O_{10}$ (A = Li, Na, K; Ln = La, Nd)," *Russian Journal of General Chemistry*, vol. 82, no. 7, pp. 1191–1196, 2012.

[11] I. Zvereva and I. Rodionov, "Photocatalytic properties of perovskite-type layered oxides," in *Perovskite: Crystallography, Chemistry and Catalytic Performance*, J. Zhang and H. Li, Eds., Nova Science Publishers, New York, 2013.

[12] A. Kudo, K. Sayama, A. Tanaka et al., "Nickel-loaded K4Nb6O17 photocatalyst in the decomposition of H_2O into H_2 and O_2: structure and reaction mechanism," *Journal of Catalysis*, vol. 120, no. 2, pp. 337–352, 1989.

[13] K. Domen, J. Yoshimura, T. Sekine, A. Tanaka, and T. Onishi, "A novel series of photocatalysts with an ion-exchangeable layered structure of niobate," *Catalysis Letters*, vol. 4, no. 4-6, pp. 339–343, 1990.

[14] J. Gopalakrishnan and V. Bhat, "$A_2Ln_2Ti_3O_{10}$ (A = potassium or rubidium; Ln = lanthanum or rare earth): a new series of layered perovskites exhibiting ion exchange," *Inorganic Chemistry*, vol. 26, no. 26, pp. 4299–4301, 1987.

[15] O. Silyukov, M. Chislov, A. Burovikhina, T. Utkina, and I. Zvereva, "Thermogravimetry study of ion exchange and hydration in layered oxide materials," *Journal of Thermal Analysis and Calorimetry*, vol. 110, no. 1, pp. 187–192, 2012.

[16] S. Byeon and H. Nam, "Neutron diffraction and FT-Raman study of ion-exchangeable layered titanates and niobates," *Chemistry of Materials*, vol. 12, no. 6, pp. 1771–1778, 2000.

[17] M. Machida, T. Mitsuyama, K. Ikeue, S. Matsushima, and M. Arai, "Photocatalytic property and electronic structure of triple-layered perovskite tantalates, $MCa_2Ta_3O_{10}$ (M = Cs, Na, H, and $C_6H_{13}NH_3$)," *The Journal of Physical Chemistry. B*, vol. 109, no. 16, pp. 7801–7806, 2005.